(19) Europäisches Patentamt
European Patent Office
Office européen des brevets

(11) EP 4 582 567 A1

(12) **EUROPEAN PATENT APPLICATION**
published in accordance with Art. 153(4) EPC

(43) Date of publication:
09.07.2025 Bulletin 2025/28

(21) Application number: **23863146.9**

(22) Date of filing: **04.09.2023**

(51) International Patent Classification (IPC):
C21D 8/12 (2006.01) ***C22C 38/00*** (2006.01)
C22C 38/10 (2006.01) ***C22C 38/14*** (2006.01)
C22C 38/60 (2006.01) ***H01F 1/147*** (2006.01)

(52) Cooperative Patent Classification (CPC):
C22C 38/00; C22C 38/10; C22C 38/14; H01F 1/147; C21D 8/12; C22C 38/60

(86) International application number:
PCT/JP2023/032247

(87) International publication number:
WO 2024/053608 (14.03.2024 Gazette 2024/11)

(84) Designated Contracting States:
AL AT BE BG CH CY CZ DE DK EE ES FI FR GB GR HR HU IE IS IT LI LT LU LV MC ME MK MT NL NO PL PT RO RS SE SI SK SM TR
Designated Extension States:
BA
Designated Validation States:
KH MA MD TN

(30) Priority: **09.09.2022 JP 2022144154**

(71) Applicant: **JFE Steel Corporation**
Tokyo 100-0011 (JP)

(72) Inventors:
- **IMAMURA, Takeshi**
  Tokyo 100-0011 (JP)
- **SHINGAKI, Yukihiro**
  Tokyo 100-0011 (JP)

(74) Representative: **Haseltine Lake Kempner LLP**
One Portwall Square
Portwall Lane
Bristol BS1 6BH (GB)

(54) **GRAIN-ORIENTED ELECTROMAGNETIC STEEL SHEET**

(57) Provided is a grain-oriented electrical steel sheet having magnetic properties that can sufficiently decrease the building factor. The grain-oriented electrical steel sheet includes a base steel sheet containing Si: 1.50 mass% to 8.00 mass%, Mn: 0.02 mass% to 1.00 mass%, and Co: 0.005 mass% to 0.050 mass%, and a base film mainly composed of forsterite, formed on the surface of the base steel sheet. Ti content in the base steel sheet and the base film as a whole is 0.0050 mass% to 0.0200 mass%. When R17 is the ratio of hysteresis loss Wh_{17} to iron loss $W_{17/50}$ when excited at 1.7 T, and R19 is the ratio of hysteresis loss Wh_{19} to iron loss $W_{19/50}$ when excited at 1.9 T, then $0.30 \leq R17 \leq R19$ is satisfied.

FIG. 1

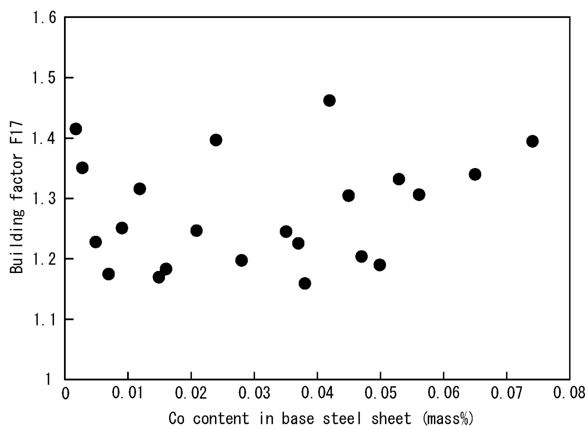

Description

TECHNICAL FIELD

[0001] The present disclosure relates to a grain-oriented electrical steel sheet advantageously utilized for an iron core of a transformer.

BACKGROUND

[0002] Grain-oriented electrical steel sheets are soft magnetic materials used as iron core materials for transformers, and have crystal microstructures in which the <001> orientation, which is an easy magnetization axis of iron, is highly accorded with the rolling direction of the steel sheets. Such texture is formed through a phenomenon called secondary recrystallization where crystal grains with {110}<001> orientation, also known as Goss orientation, grow preferentially to large sizes during purification annealing in the process of producing a grain-oriented electrical steel sheet.

[0003] A typical technique used for such a production process causes grains having Goss orientation to undergo secondary recrystallization during purification annealing using precipitates called inhibitors. For example, Patent Literature (PTL) 1 describes a method using AlN and MnS, PTL 2 describes a method using MnS and MnSe, and both of these methods have been put into industrial use.

[0004] These methods using inhibitors are useful for stable growth of secondary recrystallized grains, but for the purpose of fine particle distribution of the inhibitors into the steel, slab heating at high temperatures of 1300 °C or more is necessary to dissolve the inhibitor components in solid solution.

[0005] On the other hand, for a material containing no inhibitor components, a technique for developing crystal grains having Goss orientation through secondary recrystallization is described in PTL 3, for example. This technique eliminates impurities such as inhibitor components as much as possible and realizes grain boundary misorientation angle dependence of grain boundary energy possessed by crystal grain boundaries during primary recrystallization, thereby causing secondary recrystallization of grains having Goss orientation without using inhibitors. This effect is called the texture inhibition effect. This method does not require fine particle distribution of inhibitor into steel and therefore does not require high-temperature slab heating, which was previously essential, and is therefore a method that has significant advantages in terms of cost and maintenance.

[0006] Grain-oriented electrical steel sheets, which are mainly used as iron cores of transformers, are required to have excellent magnetization properties, in particular low iron loss. To achieve this, it is important to highly align the secondary recrystallized grains in a steel sheet to the Goss orientation and to decrease impurities in the product sheet. Further, techniques have been developed for introducing non-uniformity to the steel sheet surfaces by physical means to subdivide magnetic domain width for less iron loss, namely, magnetic domain refining techniques. For example, PTL 4 proposes a technique of irradiating a steel sheet after final annealing with a laser to introduce high-dislocation density regions into a surface layer of the steel sheet, thereby narrowing magnetic domain widths and decreasing iron loss of the steel sheet. Further, PTL 5 proposes a technique of controlling magnetic domain widths by irradiation with an electron beam.

[0007] The highly-aligned orientation after secondary recrystallization to the Goss orientation and the decrease in impurities in the product sheet result in lower hysteresis loss. In contrast, eddy current loss is mainly decreased when magnetic domain refining techniques are applied.

CITATION LIST

Patent Literature

[0008]

PTL 1: JP S40-15644 B2
PTL 2: JP S51-13469 B2
PTL 3: JP 2000-129356 A
PTL 4: JP S57-2252 B2
PTL 5: JP H06-72266 B2

SUMMARY

(Technical Problem)

[0009] As mentioned above, grain-oriented electrical steel sheets are mainly used as the iron cores of transformers. In general, there is a discrepancy between the iron loss value of a transformer iron core and the iron loss value of a grain-oriented electrical steel sheet that is a material of the iron core, and the iron loss is greater for the transformer iron core. The iron loss ratio of the two (the iron loss of the transformer iron core divided by the iron loss value of the material) is called the building factor. That is, even when the iron loss of the material is low, when the building factor is high, the iron loss of the transformer iron core is large, creating a problem of insufficient performance. In the carbon-neutral era, what needs to be decreased is the iron loss of the final product, the transformer. No matter how low the iron loss of the material is, it is meaningless when the building factor is high. The building factor affects not only transformer design but also material properties, and therefore there is a demand to lower the building factor as well as the iron loss of the material.

[0010] That is, it would be helpful to provide a grain-oriented electrical steel sheet having magnetic properties that can sufficiently decrease the building factor.

(Solution to Problem)

[0011] As a result of extensive studies, the inventors have discovered that a grain-oriented electrical steel sheet that can obtain a low building factor can be produced by controlling, within certain ranges, the Co content in a base steel sheet, on which a base film mainly composed of forsterite is formed, and the Ti content in the grain-oriented electrical steel sheet with the base film formed thereon.

[0012] The following describes the experiments that successfully led to the present disclosure.

<Experiment 1>

[0013] Mainly in order to vary the Co content, steel slabs were produced by continuous casting, containing, in mass%, C: 0.050 % to 0.081 %, Si: 3.15 % to 3.31 %, Mn: 0.07 % to 0.10 %, Al: 0.020 % to 0.025 %, N: 0.0069 % to 0.0085 %, S: 0.0011 % to 0.0031 %, Sb: 0.025 % to 0. 036 %, Co: 0 % to 0.123 %, and Ti: 0.0080 % to 0.0090 %, with the balance being Fe and inevitable impurity. After slab heating and soaking at 1400 °C for 20 min, the slabs were hot rolled to a thickness of 2.4 mm. Subsequently, hot-rolled sheet annealing was carried out at 1000 °C for 30 s in an N_2 atmosphere. Next, cold rolling was carried out to a thickness of 1.5 mm, followed by intermediate annealing at 1000 °C for 100 s in a 25 % H_2 - 75 % N_2 atmosphere. Subsequently, cold rolling was carried out to a thickness of 0.23 mm, followed by decarburization annealing at 850 °C for 150 s in a wet atmosphere of 50 % H_2 - 50 % N_2 with a dew point of 50 °C. Next, after the decarburization annealing, to the surface of each base steel sheet, an annealing separator consisting mainly of MgO was applied, and purification annealing was carried out by holding at 1200 °C for 10 h. At this time, the heating rate to 1200 °C was 20 °C/h. Further, during the heating process, an N_2 atmosphere was used from room temperature to 700 °C, an atmosphere in which the mixing ratio of N_2 and H_2 was varied was used from 700 °C to 1100 °C, and an H_2 atmosphere was used from 1100 °C to 1200 °C. Further, an H_2 atmosphere was used during the hold time, and an Ar atmosphere was used during cooling. In this way, samples were obtained where a base film consisting mainly of forsterite (hereinafter also referred to as forsterite film) was formed on the surface of each base steel sheet.

[0014] For the samples thus obtained, the iron loss $W_{17/50}$ (iron loss when excited at 50 Hz up to 1.7 T) and $W_{19/50}$ (iron loss when excited at 50 Hz up to 1.9 T), hysteresis loss Wh_{17} (hysteresis loss when excited up to 1.7 T) and Wh_{19} (hysteresis loss when excited up to 1.9 T) were measured by the method specified in Japanese Industrial Standard JIS C2550-1.

[0015] Further, to measure the amount of Co in each base steel sheet, a portion of the obtained sample was immersed in a 10 % hydrochloric acid aqueous solution at 80 °C for 180 s to remove the forsterite film, and the amount of Co was measured by the method specified in JIS G1222.

[0016] Then, from each of the obtained samples, a three-phase three-leg model transformer simulating a transformer was fabricated having an external shape of 500 mm square and a sheet width of 100 mm for each leg and each yoke, and model transformer iron loss $WT_{17/50}$ (transformer iron loss when excited at 50 Hz to 1.7 T) was measured. The number of stacked sheets of each sample was 50, with two sheets stacked alternately. The building factor F17 of the model transformer was then calculated as the model transformer iron loss $WT_{17/50}$ divided by the sample iron loss $W_{17/50}$ ($WT_{17/50}/W_{17/50}$). The relationship between the building factor F17 and the amount of Co in the base steel sheet is illustrated in FIG. 1.

[0017] The results illustrated in FIG. 1 indicate no clear correlation between the building factor F17 and Co content. However, it can be read from FIG. 1 that the building factor F17 is divided into good values of 1.25 or less and high values of 1.30 or more.

[0018] The relationship between iron loss and hysteresis loss of the samples was examined to see whether this difference could be explained. As a result, when R17 is the ratio of hysteresis loss Wh_{17} to iron loss $W_{17/50}$ when excited at 1.7 T, and R19 is the ratio of hysteresis loss Wh_{19} to iron loss $W_{19/50}$ when excited at 1.9 T, the inventors found that there are two groups, group A having the relationship $0.30 \leq R17 \leq R19$, and the other group B. FIG. 2 is the result of extracting and redrawing only the group A of the data in FIG. 1.

[0019] The results illustrated in FIG. 2 indicate that results belonging to group A, that is, having the relationship 0.30 ≤ R17 ≤ R19, in a Co content range from 0.005 % to 0.050 %, indicate a good building factor of 1.25 or less.

<Experiment 2>

[0020] Steel slabs were produced by continuous casting, containing, in mass%, C: 0.037 %, Si: 3.05 %, Mn: 0.18 %, Al: 0.009 %, N: 0.0036 %, Se: 0.007 %, Sn: 0.062 %, and Co: 0.0080 %, with the balance being Fe and inevitable impurity. After slab heating and soaking at 1300 °C for 30 min, the slabs were hot rolled to a thickness of 2.2 mm. Subsequently, hot-rolled sheet annealing was carried out at 1100 °C for 30 s in an N_2 atmosphere. Next, cold rolling was carried out to a thickness of 0.23 mm, followed by decarburization annealing at 840 °C for 120 s in a wet atmosphere of 40 % H_2 - 60 % N_2 with a dew point of 40 °C. Next, after the decarburization annealing, to the surface of each base steel sheet, an annealing separator containing TiO_2 in various amounts ranging from 0 to 15 parts by mass relative to MgO was applied, and purification annealing was carried out by holding at 1220 °C for 5 h. At this time, the heating rate to 1220 °C was 15 °C/h. Further, during the heating process, an N_2 atmosphere was used from room temperature to 700 °C, an atmosphere in which the mixing ratio of N_2 and H_2 was varied was used from 700 °C to 1100 °C, and an H_2 atmosphere was used from 1100 °C to 1220 °C. Further, an H_2 atmosphere was used during the hold time, and an Ar atmosphere was used during cooling. In this way, samples were obtained where a base film consisting mainly of forsterite (hereinafter also referred to as forsterite film) was formed on the surface of each base steel sheet.

[0021] For the samples thus obtained, the iron losses $W_{17/50}$ and $W_{19/50}$ and hysteresis losses Wh_{17} and Wh_{19} were measured as in Experiment 1, using the method specified in JIS C2550-1.

[0022] Further, the Ti content in each steel sheet with the forsterite film was measured by the method specified in JIS G1223.

[0023] Further, to measure the amount of Co in each base steel sheet, a portion of the obtained sample was immersed in a 10 % hydrochloric acid aqueous solution at 80 °C for 180 s to remove the forsterite film, and the amount of Co was measured by the method specified in JIS G1222. As a result, the Co content was 0.0080 %, which was equivalent to that of the steel slab.

[0024] Further, as in Experiment 1, when R17 is the ratio of hysteresis loss Wh_{17} to iron loss $W_{17/50}$ when excited at 1.7 T, and R19 is the ratio of hysteresis loss Wh_{19} to iron loss $W_{19/50}$ when excited at 1.9 T, the results were divided into two groups, group A having the relationship 0.30 ≤ R17 ≤ R19, and the other group B. The relationship between the Ti content in steel sheets with forsterite film and belonging to group A or group B is illustrated in FIG. 3.

[0025] The results illustrated in FIG. 3 indicate that when the Ti content in the steel sheet with forsterite film is at least 0.0039 % and at most 0.0200 %, the steel sheet tends to belong to group A.

[0026] Further, as in Experiment 1, three-phase three-leg model transformers were fabricated, each having an external shape of 500 mm square and a sheet width of 100 mm for each leg and each yoke, and model transformer iron loss $WT_{17/50}$ (transformer iron loss when excited at 50 Hz to 1.7 T) was measured. The building factor F17 of the model transformer was then calculated as the model transformer iron loss $WT_{17/50}$ divided by the sample iron loss $W_{17/50}$ ($WT_{17/50}/W_{17/50}$). The relationship between the building factor F17 and the Ti content in the steel sheet with forsterite film is illustrated in FIG. 4.

[0027] The results illustrated in FIG. 4 indicate that when the Ti content in the steel sheet with forsterite film is less than 0.0050 %, the building factor F17 is high even when the sheet belongs to group A. In summary, the inventors found that the building factor is low and good when the Ti content in the steel sheet with forsterite film is from 0.0050 % to 0.0200 %. This essentially means that it is good for a certain amount of Ti to be present in the forsterite film.

[0028] The mechanism by which the building factor of the model transformer becomes better depending on the Co content in the base steel sheet and the Ti content in the steel sheet with a base film that is mainly forsterite, as described above, is not clear, but the inventors consider the following to be possible.

[0029] The yoke and legs of the transformer have a certain width, and therefore the magnetic path differs in distance between the inside and the outside, like a track in athletics. Therefore, during excitation, the magnetic flux tends to be biased toward the inner side where the magnetic path is short. Even when the entire steel sheet is excited to 1.7 T, the magnetic flux density on the inner side exceeds that. Therefore, it may be that the more favorable the high magnetic field properties, the better the transformer properties such as the building factor. When Co is solute in iron, it is expected that the saturation magnetic flux density of the iron increases and high magnetic field properties improve, and this may be why the building factor improved. However, through Experiments 1 and 2, there were two cases where the building factor was not good, even when Co was added.

[0030] The first case was when the ratio of the hysteresis loss Wh_{17} to the iron loss $W_{17/50}$ when excited at 1.7 T, that is, R17, and the ratio of the hysteresis loss Wh_{19} to the iron loss $W_{19/50}$ when excited at 1.9 T, that is, R19, did not satisfy the relationship 0.30 ≤ R17 ≤ R19. Detailed investigation revealed that R17 was less than 0.30 in the majority of cases. Hysteresis loss is highly correlated with B_8 and the same B_8 is not expected to vary significantly, and therefore the above is considered a case of extremely large eddy current loss. In a transformer, even when excited with a sinusoidal waveform, a high-harmonic component is superimposed and the waveform is distorted, which may increase eddy current loss, which is highly frequency-dependent. Therefore, a high eddy current loss ratio may increase the building factor.

[0031] The second case was when the Ti content in the steel sheet with forsterite film was less than 0.0050 mass% or more than 0.0200 mass%. Although only a hypothesis, the presence of a certain amount of Ti in the forsterite film may improve film properties. For example, an increase in film tension may refine the magnetic domain and decrease eddy current losses. In such a case, the eddy current loss ratio is lowered, contrary to the case of R17 and R19 above, and therefore the building factor may be decreased.

[0032] A production technique for a grain-oriented electrical steel sheet containing Co is described in JP 2021-509149 A. However, the literature mentions a technique to improve the magnetic properties of the electrical steel sheet itself, which is completely different from the present disclosure, which decreases the building factor by combination with a technology to include Ti in the forsterite film.

[0033] The present disclosure is based on the above discoveries. Primary features of the present disclosure are as follows.

1. A grain-oriented electrical steel sheet comprising a base steel sheet containing Si: 1.50 mass% to 8.00 mass%, Mn: 0.02 mass% to 1.00 mass%, and Co: 0.005 mass% to 0.050 mass%, and a base film mainly composed of forsterite, formed on the surface of the base steel sheet, wherein

   Ti content in the base steel sheet and the base film as a whole is 0.0050 mass% to 0.0200 mass%, and the following expression (1) is satisfied, where R17 is the ratio of hysteresis loss Wh_{17} to iron loss $W_{17/50}$ when excited at 1.7 T and R19 is the ratio of hysteresis loss Wh_{19} to iron loss $W_{19/50}$ when excited at 1.9 T,

$$0.30 \leq R17 \leq R19 \qquad \ldots(1).$$

2. The grain-oriented electrical steel sheet according to 1, above, wherein Ti content in the base steel sheet is 0.0030 mass% or less.
3. The grain-oriented electrical steel sheet according to 1 or 2, above, further comprising an insulating coating on the surface of the base film.
4. The grain-oriented electrical steel sheet according to any one of 1 to 3, above, wherein the base steel sheet further contains one or more selected from the group consisting of Sn: 0.500 mass% or less, Cr: 0.500 mass% or less, Cu: 0.50 mass% or less, Ni: 0.50 mass% or less, Bi: 0.500 mass% or less, P: 0.500 mass% or less, Sb: 0.500 mass% or less, Mo: 0.500 mass% or less, B: 25.0 mass ppm or less, Nb: 0.020 mass% or less, V: 0.020 mass% or less, As: 0.0200 mass% or less, Zn: 0.020 mass% or less, Pb: 0.0100 mass% or less, W: 0.0100 mass% or less, Ga: 0.0050 mass% or less, and Ge: 0.0050 mass% or less.

(Advantageous Effect)

[0034] According to the present disclosure, a grain-oriented electrical steel sheet having magnetic properties that can sufficiently decrease the building factor can be provided.

BRIEF DESCRIPTION OF THE DRAWINGS

[0035] In the accompanying drawings:

FIG. 1 is a graph illustrating a relationship between Co content of base steel sheets and building factor F17, with respect to Experiment 1;

FIG. 2 is a graph illustrating the relationship between Co content of base steel sheets and building factor F17 (where only group A is extracted), with respect to Experiment 1;

FIG. 3 is a graph illustrating a relationship between Ti content of steel sheets with forsterite film and belonging to group A or group B, with respect to Experiment 2; and

FIG. 4 is a graph illustrating a relationship between Ti content of steel sheets with forsterite film and building factor F17, with respect to Experiment 2.

DETAILED DESCRIPTION

[0036] Reasons for limitations on the primary features of the present disclosure are explained below. First, the amount of each element (chemical composition) in the base steel sheet of the grain-oriented electrical steel sheet is explained. Hereinafter, "%" and "ppm" designations for chemical composition refer to "mass%" and "mass ppm," respectively, unless otherwise noted.

Si: 1.50 % to 8.00 %

[0037] Si is an element necessary for increasing the specific resistance of steel and decreasing iron loss. Further, Si is an element necessary for forming forsterite film in the steel sheet according to the present disclosure. However, Si content of less than 1.50 % is ineffective, and the Si content exceeding 8.00 % degrades steel workability and makes rolling difficult. Accordingly, the Si content is limited to 1.50 % to 8.00 %. The Si content is preferably 2.50 % or more. The Si content is preferably 4.50 % or less.

Mn: 0.02 % to 1.00 %

[0038] Mn is an element necessary for good hot workability. However, Mn content of less than 0.02 % is ineffective, and the Mn content exceeding 1.00 % decreases product sheet magnetic flux density. The Mn content is therefore from 0.02 % to 1.00 %. The Mn content is preferably 0.04 % or more. The Mn content is preferably 0.20 % or less.

Co: 0.005 % to 0.050 %

[0039] For the reasons mentioned above, it is essential that Co content be in the range from 0.005 % to 0.050 %. The Co content is preferably 0.006% or more. The Co content is more preferably 0.008 % or more. Further, the Co content is preferably 0.020 % or less. The Co content is more preferably 0.015 % or less.

[0040] In addition to the basic components (Si, Mn, and Co) described above, the base steel sheet of the grain-oriented electrical steel sheet may contain C (for example, 0.020 % to 0.100 %), may contain Al (for example, 0.002 % to 0.040 %), and may contain N (for example, 0.002 % to 0.015 %). Further, the base steel sheet may optionally contain S (for example, 0.020 % or less) and/or Se (for example, 0.040 % or less). In addition to the above components, the base steel sheet of the grain-oriented electrical steel sheet may contain the components (elements) described below as required.

[0041] Specifically, for the purpose of improving magnetic properties, the base steel sheet may contain one or more selected from the group consisting of Sn: (more than 0 %) 0.500 % or less, Cr: (more than 0 %) 0.500 % or less, Cu: (more than 0 %) 0.50 % or less, Ni: (more than 0 %) 0.50 % or less, Bi: (more than 0 %) 0.500 % or less, P: (more than 0 %) 0.500 % or less, Sb (more than 0 %) 0.500 % or less, Mo: (more than 0 %) 0.500 % or less, B: (more than 0 ppm) 25.0 ppm or less, Nb: (more than 0 %) 0.020 % or less, V: (more than 0 %) 0.020 % or less, As: (more than 0 %) 0.0200 % or less, Zn: (more than 0 %) 0.020 % or less, Pb: (more than 0 %) 0.0100 % or less, W: (more than 0 %) 0.0100 % or less, Ga: (more than 0 %) 0.0050 % or less, and Ge: (more than 0 %) 0.0050 % or less.

[0042] That is, each of the above elements may be contained in the base steel sheet in a range up to the upper limit described above to further improve magnetic properties. When the amount of each element added (content) exceeds the above upper limit, the development of secondary recrystallized grains may be suppressed and magnetic properties may deteriorate. Although there is no particular need to limit a lower limit of each element, each element is preferably contained in the following range.

[0043] Sn: 0.005 % or more, Cr: 0.005 % or more, Cu: 0.01 % or more, Ni: 0.01 % or more, Bi: 0.005 % or more, P: 0.005 % or more, Sb: 0.005 % or more, Mo: 0.005 % or more, B: 0.1 ppm or more, Nb: 0.001 % or more, V: 0.001 % or more, As: 0.0010 % or more, Zn: 0.001 % or more, Pb: 0.0001 % or more, W: 0.0010 % or more, Ga: 0.0001 % or more, and Ge: 0.0001 % or more.

[0044] In the base steel sheet, the balance other than the components (elements) mentioned above is Fe and inevitable impurity.

[0045] The chemical composition described above is the chemical composition in the base steel sheet, that is, without considering the base film, which is mainly composed of forsterite. Further, according to the present disclosure, Ti content in the steel sheet with the base film mainly composed of forsterite, that is, the Ti content in the base steel sheet and the base film as a whole, is limited to 0.0050 % to 0.0200 % for the reasons mentioned above. The Ti content in the base steel sheet and the base film as a whole is preferably 0.0060 % or more. The Ti content is preferably 0.0150 % or less.

[0046] The term "mainly composed" with respect to the base film refers to the component having the greatest mass among the components of the base film.

[0047] Here, in limiting the Ti content in the steel sheet with the base film to 0.0050 % to 0.0200 %, the Ti content in the base steel sheet is preferably 0.0030% or less. When the Ti content in the base steel sheet is 0.0030 % or less, significant degradation of iron loss due to the formation of Ti precipitates in steel can be suppressed. On the other hand, the Ti content in the steel sheet with the base film is 0.0050 % or more. This is because, as mentioned above, a certain amount of Ti in the forsterite film may improve film properties and decrease eddy current loss, but when the Ti content is less than 0.0050 %, the effect is estimated to be poor.

[0048] Further, as mentioned above, the present disclosure requires limiting the range of a set of parameters calculated from hysteresis loss and iron loss of the product steel sheet. That is, the ratio R17 (=$Wh_{17}/W_{17/50}$) of hysteresis loss Wh_{17} to iron loss $W_{17/50}$ when excited at 1.7 T and the ratio R19 (=$Wh_{19}/W_{19/50}$) of hysteresis loss Wh_{19} to iron loss $W_{19/50}$ when excited at 1.9 T need to satisfy the relationship $0.30 \leq R17 \leq R19$. These values can be measured by the method specified in JIS C2550-1. In order to match the hysteresis loss with the iron loss at 50 Hz, the hysteresis loss can be calculated by multiplying the energy loss of the iron core in one cycle of the hysteresis loop by 50, which is the excitation frequency.

[0049] The following describes a method of producing the grain-oriented electrical steel sheet according to the present disclosure. The method of production may use a typical method for producing an electrical steel sheet. For example, molten steel prepared to have defined components may be made into a slab by typical ingot casting or continuous casting, or made into a thin slab or thinner cast steel having a thickness of 100 mm or less by direct casting. Molten steel may be produced by either a blast furnace or an electric furnace steelmaking process. The various components that may be contained in the base steel sheet are difficult to add during the process, and therefore adding them at the molten steel stage is preferred. The slab may be heated and hot rolled by a typical method or hot rolled directly after casting without heating. When heating, a chemical composition containing a small amount of inhibitor components does not require high-temperature annealing for dissolving the inhibitor, and therefore a low temperature of 1300 °C or less is effective for cost-reduction purposes. When heating, the temperature is preferably 1250 °C or less.

[0050] Subsequently, hot-rolled sheet annealing may be carried out as required. The temperature of hot-rolled sheet annealing is preferably about 950 °C to 1150 °C. When the temperature is 950 °C or more, residual un-recrystallized portions can be sufficiently suppressed, and when the temperature is 1150 °C or less, excessive coarsening of grain size after annealing can be suppressed and the subsequent primary recrystallized texture can be made more favorable. The temperature of hot-rolled sheet annealing is preferably 1000 °C or more. The temperature of hot-rolled sheet annealing is preferably 1100 °C or less.

[0051] The steel sheet after the hot rolling or hot-rolled sheet annealing is subjected to cold rolling once, or twice or more with intermediate annealing carried out therebetween, to obtain a cold-rolled sheet having a final sheet thickness. The annealing temperature for intermediate annealing is preferably in a range from 900 °C to 1200 °C. When the temperature is 900 °C or more, the recrystallized grain becoming too fine after intermediate annealing can be well suppressed, and further, a decrease in magnetic properties of the product sheet due to a decrease in Goss nuclei in the primary recrystallized texture can be well suppressed. On the other hand, when the temperature is 1200 °C or less, as with hot-rolled sheet annealing, excessive coarsening of crystal grains can be suppressed and the primary recrystallized texture of the uniformly-sized grains can be made better.

[0052] The cold-rolled sheet having a final sheet thickness is then subjected to primary recrystallization annealing that also serves as decarburization annealing. The annealing temperature for this primary recrystallization annealing is, when accompanied by decarburization annealing and from the viewpoint of allowing the decarburization reaction to proceed rapidly, preferably in a range from 800 °C to 900 °C, and the atmosphere is preferably a wet atmosphere.

[0053] Subsequently, an annealing separator mainly composed of MgO is applied, followed by purification annealing to develop a secondary recrystallized texture and form a forsterite film. Here, mainly composed of MgO means that MgO content is 75 mass% or more.

[0054] Further, the addition of a Ti compound to the annealing separator and the introduction of an N_2 atmosphere during purification annealing, as described below, effectively allow Ti to be present in the forsterite film. However, Ti may be made to be present in the forsterite film in other ways.

[0055] Subsequently, secondary recrystallization annealing (purification annealing) is carried out. This purification annealing is preferably carried out at 800 °C or more for the development of secondary recrystallization, and from the purification point of view, the temperature is preferably raised to a holding temperature of 1100 °C or more. The holding temperature is more preferably 1180 °C or more. Here, the longer the hold time, the more purification progresses, but shape degradation may occur due to high-temperature creep, and therefore the hold time is preferably at least 3 h and at most 15 h. After the purification annealing, water washing, brushing, or pickling is preferably carried out to remove adhered annealing separator. Further, from the viewpoint of obtaining desired iron loss properties, in the heating process of the purification annealing, it is preferable to use an N_2 atmosphere up to a first intermediate temperature (for example, a temperature selected from the range from 600 °C to 800 °C), a mixed N_2 and H_2 atmosphere from the first intermediate temperature to a second intermediate temperature (for example, a temperature selected from the range from 1050 °C to 1150 °C), and an H_2 atmosphere from the second intermediate temperature to the holding temperature.

[0056] Subsequently, flattening annealing is carried out for shape adjustment, which is effective for iron loss reduction. In the case of using the steel sheet in a stack, applying an insulating coating to the steel sheet surface before or after the flattening annealing is effective for reducing iron loss. As the insulating coating, a film that can impart tension to the steel sheet to reduce iron loss is preferable. A method of tension film coating application through a binder, or coating by depositing an inorganic substance onto the steel sheet surface layer by physical vapor deposition or chemical vapor deposition is preferable, as these methods have excellent coating adhesion and a considerable iron loss reduction effect.

EXAMPLES

[0057] The present disclosure is described in detail below by reference to examples. However, the present disclosure is not limited to these examples.

(Examples 1)

[0058] Steel slab A - C: 0.070 %, Si: 3.55 %, Mn: 0.07 %, Al: 0.0080 %, N: 0.0050 %, Co: 0.012 %, Mo: 0.026 %, Ti: 0.025 %, with the balance being Fe and inevitable impurity.
[0059] Steel slab B - C: 0.072 %, Si: 3.51 %, Mn: 0.07 %, Al: 0.0080 %, N: 0.0047 %, Co: 0.011 %, Mo: 0.025 %, Ti: 0.0025 %, with the balance being Fe and inevitable impurity.
[0060] Steel slab C - C: 0.072 %, Si: 3.49 %, Mn: 0.07 %, Al: 0.0090 %, N: 0.0051 %, Co: 0.002 %, Mo: 0.025 %, Ti: 0.024 %, with the balance being Fe and inevitable impurity.
[0061] Steel slab D - C: 0.068 %, Si: 3.48 %, Mn: 0.07 %, Al: 0.0090 %, N: 0.0050 %, Co: 0.008 %, Mo: 0.022 %, Ti: 0.0010 %, with the balance being Fe and inevitable impurity.
[0062] Each of the steel slabs A to D described above was produced by continuous casting, and after slab heating to soak at 1200 °C for 40 min, the slabs were hot rolled to a thickness of 2.2 mm. Hot-rolled sheet annealing was then carried out at 1000 °C for 60 s in an N_2 atmosphere. Next, cold rolling was carried out to a thickness of 0.23 mm, followed by decarburization annealing at 850 °C for 90 s in a wet atmosphere of 60 % H_2 - 40 % N_2 with a dew point of 60 °C.
[0063] Next, after the decarburization annealing, to the surface of each base steel sheet, an annealing separator consisting mainly of MgO (MgO: 97 mass%) was applied, and purification annealing was carried out by holding at 1100 °C for 25 h, then holding at 1200 °C for 10 h. During the heating process, an N_2 atmosphere was used from room temperature to 700 °C, an atmosphere in which the mixing ratio of N_2 and H_2 was varied was used from 700 °C to 1100 °C, and an H_2 atmosphere was used from 1100 °C (start of holding) to 1200 °C (end of holding). Further, an Ar atmosphere was used during cooling.
[0064] The Ti content (the total Ti content of the base steel sheet and the base film) of the obtained samples, that is, steel sheets with a mainly forsterite base film, was measured according to the method specified in JIS G1223. The results are listed in Table 1.
[0065] On the base film of each of the above steel sheets, an insulating coating consisting mainly of magnesium phosphate and silica was applied and formed. For the samples thus obtained, the iron loss $W_{17/50}$ (iron loss when excited at 50 Hz up to 1.7 T) and $W_{19/50}$ (iron loss when excited at 50 Hz up to 1.9 T), and hysteresis loss Wh_{17} (hysteresis loss when excited up to 1.7 T) and Wh_{19} (hysteresis loss when excited up to 1.9 T) were measured according to the method specified in Japanese Industrial Standard JIS C2550-1. $Wh_{17}/W_{17/50}$ (that is, R17), and $Wh_{19}/W_{19/50}$ (that is, R19) are listed in Table 1.
[0066] Further, to measure the Co content and Ti content in each base steel sheet, a portion of the obtained sample was immersed in a 10 % hydrochloric acid aqueous solution at 80 °C for 180 s to remove the base film, and the Co content and Ti content were measured by the methods specified in JIS G1222 and JIS G1223. The measurement results are listed in Table 1.
[0067] Then, from each of the samples with the insulating coating, a three-phase three-leg model transformer simulating a transformer was fabricated having an external shape of 500 mm square and a sheet width of 100 mm for each leg and each yoke, and model transformer iron loss $WT_{17/50}$ (transformer iron loss when excited at 50 Hz to 1.7 T) was measured. The number of stacked sheets of each sample was 50, with two sheets stacked alternately. The building factor F17 of the model transformer was then calculated as the model transformer iron loss $WT_{17/50}$ divided by the sample iron loss $W_{17/50}$ ($WT_{17/50}/W_{17/50}$). The results are listed in Table 1.

[Table 1]

[0068]

Table 1

No.	Slab type	Ti content in steel sheet with base film (%)	Ti content in base steel sheet (%)	Co content in base steel sheet (%)	R17	R19	Building factor F17	Remarks
1	A	0.0180	0.0015	0.012	0.39	0.51	1.18	Example
2	B	<u>0.0024</u>	0.0020	0.011	<u>0.28</u>	0.40	1.41	Comparative Example

(continued)

No.	Slab type	Ti content in steel sheet with base film (%)	Ti content in base steel sheet (%)	Co content in base steel sheet (%)	R17	R19	Building factor F17	Remarks
3	C	0.0190	0.0018	<u>0.002</u>	0.35	0.49	1.35	Comparative Example
4	D	<u>0.0018</u>	0.0015	0.008	0.34	0.50	1.32	Comparative Example

[0069] It is clear from Table 1 that good iron loss properties (building factor) were obtained for the sample according to the present disclosure (grain-oriented electrical steel sheet).

(Examples 2)

[0070] Steel slabs containing the components listed in Table 2, with the balance being Fe and inevitable impurity, were prepared by continuous casting. Each steel slab was subjected to slab heating to soak at 1410 °C for 20 min, and hot rolled to obtain a hot-rolled sheet having a thickness of 2.4 mm. Hot-rolled sheet annealing was then carried out at 1100 °C for 20 s in an N_2 atmosphere. Next, cold rolling was carried out to a thickness of 1.5 mm, followed by intermediate annealing at 900 °C for 100 s in a 25 % H_2 - 75 % N_2 atmosphere. Subsequently, cold rolling was carried out to a thickness of 0.23 mm, followed by decarburization annealing at 825 °C for 150 s in a wet atmosphere of 40 % H_2 - 60% N_2 with a dew point of 45 °C.

[Table 2]

[0071]

Table 2

No.	Slab									
	Type	Si	Mn	Co	C	Al	N	S	Se	Other components
		mass%	mass%	mass%	mass%	mass%	mass%	mass%	mass%	mass%
5	E	3.26	0.52	0.005	0.041	0.033	0.0033	0.0023	-	-
6	F	3.26	0.12	0.011	0.042	0.009	0.0081	-	0.005	-
7	G	2.22	0.18	0.045	0.056	0.011	0.0028	0.0009	-	-
8	H	<u>1.16</u>	0.20	0.009	0.067	0.014	0.0049	0.0015	-	-
9	I	<u>5.25</u>	0.24	0.011	0.027	0.018	0.0048	0.0017	0.016	-
10	J	3.02	<u>0.01</u>	0.017	0.038	0.012	0.0045	0.0018	-	-
11	K	3.28	<u>1.05</u>	0.010	0.045	0.011	0.0047	0.0028	0.022	-
12	L	2.98	0.24	<u>0.002</u>	0.071	0.023	0.0026	0.0034	0.023	-
13	M	3.20	0.18	<u>0.065</u>	0.030	0.013	0.0078	0.0023	0.002	-
14	N	3.41	0.14	0.007	0.058	0.007	0.0033	0.0015	-	Sn:0.350, Ni:0.23, Bi:0.006, V:0.002
15	O	3.00	0.22	0.016	0.047	0.018	0.0036	0.0010	0.007	Cr:0.012, As:0.0080, Ge:0.0040, P:0.010, Ni:0.02

(continued)

No.	Slab									
	Type	Si	Mn	Co	C	Al	N	S	Se	Other components
		mass%	mass%	mass%	mass%	mass%	mass%	mass%	mass%	mass%
16	P	3.09	0.20	0.018	0.025	0.030	0.0034	-	-	P:0.120, Sb:0.007, Nb:0.002, Cr:0.27
17	Q	3.41	0.22	0.015	0.080	0.014	0.0082	0.0011	-	W:0.0020, Zn:0.007, Pb:0.0080, Ti:0.0100
18	R	3.39	0.21	0.010	0.076	0.030	0.0035	0.0033	0.007	Sn:0.009, B:21.2 ppm, Cu:0.35, Ga:0.0040
19	S	3.46	0.15	0.010	0.070	0.009	0.0038	0.0033	0.011	Cr:0.41, Bi:0.170, Pb:0.0004. Mo:0.250
20	T	3.21	0.11	0.010	0.033	0.008	0.0031	0.0028	-	Cu:0.02, As:0.0015, Zn:0.012, W:0.0080
21	U	3.35	0.06	0.011	0.037	0.012	0.0072	0.0022	0.018	Sb:0.330, Ga:0.0003, Ge:0.0003, B:0.3 ppm
22	V	4.41	0.14	0.016	0.082	0.027	0.0078	0.0013	-	Mo:0.008, Ti:0.0008, V:0.011, Nb:0.012

[0072] Next, after the decarburization annealing, to the surface of each base steel sheet, an annealing separator consisting mainly of MgO (MgO: 88 mass%) was applied. For the annealing separator, TiO_2 powder was put into warm water at 50 °C and stirred for 24 h, and 5 parts by mass of the resulting superhydrated TiO_2 was added to the MgO powder.

[0073] Further, purification annealing was carried out by holding at 1200 °C for 10 h. At this time, the heating rate to 1200 °C was 15 °C/h. Further, during the heating process, an N_2 atmosphere was used from room temperature to 700 °C, an atmosphere in which the mixing ratio of N_2 and H_2 was varied was used from 700 °C to 1100 °C, and an H_2 atmosphere was used from 1100 °C to 1200 °C. Further, an H_2 atmosphere was used during the hold time, and an Ar atmosphere was used during cooling.

[0074] The Ti content (the total Ti content of the base steel sheet and the base film) of the obtained samples, that is, steel sheets with a mainly forsterite base film, was measured according to the method specified in JIS G1223. The measurement results are listed in Table 3.

[0075] On the base film of each of the above steel sheets, an insulating coating consisting mainly of magnesium phosphate and silica was applied and formed. For the samples thus obtained, the iron loss $W_{17/50}$ (iron loss when excited at 50 Hz up to 1.7 T) and $W_{19/50}$ (iron loss when excited at 50 Hz up to 1.9 T), and hysteresis loss Wh_{17} (hysteresis loss when excited up to 1.7 T) and Wh_{19} (hysteresis loss when excited up to 1.9 T) were measured according to the method specified in Japanese Industrial Standard JIS C2550-1. $Wh_{17}/W_{17/50}$ (that is, R17), and $Wh_{19}/W_{19/50}$ (that is, R19) are listed in Table 3.

[0076] Further, to measure the Co content and Ti content in each base steel sheet, a portion of the obtained sample was immersed in a 10 % hydrochloric acid aqueous solution at 80 °C for 180 s to remove the base film, and the Co content and Ti content were measured by the methods specified in JIS G1222 and JIS G1223. The measurement results are listed in Table 3.

[0077] Then, from each of the samples with the insulating coating, a three-phase three-leg model transformer simulating a transformer was fabricated having an external shape of 500 mm square and a sheet width of 100 mm for each leg and each yoke, and model transformer iron loss $WT_{17/50}$ (transformer iron loss when excited at 50 Hz to 1.7 T) was measured. The number of stacked sheets of each sample was 50, with two sheets stacked alternately. The building factor F17 of the model transformer was then calculated as the model transformer iron loss $WT_{17/50}$ divided by the sample iron loss $W_{17/50}$ ($WT_{17/50}/W_{17/50}$). The results are listed in Table 3.

[Table 3]

[0078]

Table 3

No.	Slab type	Ti content in steel sheet with base film (%)	Ti content in base steel sheet (%)	Co content in base steel sheet (%)	R17	R19	Building factor F17	Remarks
5	E	0.015	0.0034	0.005	0.36	0.48	1.23	Example
6	F	0.011	0.0016	0.011	0.41	0.61	1.17	Example
7	G	0.009	0.0023	0.045	0.36	0.52	1.09	Example
8	H	0.014	0.0008	0.009	0.38	0.46	1.68	Comparative Example
9	I	0.012	0.0019	0.011	0.37	0.44	1.33	Comparative Example
10	J	No secondary recrystallization						Comparative Example
11	K	No secondary recrystallization						Comparative Example
12	L	0.009	0.0016	0.002	0.37	0.44	1.32	Comparative Example
13	M	0.014	0.0027	0.065	0.36	0.55	1.45	Comparative Example
14	N	0.008	0.0021	0.007	0.43	0.54	1.18	Example
15	O	0.012	0.0020	0.016	0.36	0.54	1.15	Example
16	P	0.017	0.0030	0.018	0.42	0.45	1.19	Example
17	Q	0.011	0.0026	0.015	0.37	0.45	1.19	Example
18	R	0.013	0.0029	0.010	0.37	0.46	1.12	Example
19	S	0.009	0.0014	0.010	0.34	0.50	1.15	Example
20	T	0.008	0.0018	0.010	0.38	0.45	1.20	Example
21	U	0.018	0.0033	0.011	0.43	0.65	1.11	Example
22	V	0.019	0.0016	0.016	0.39	0.48	1.22	Example

[0079] It is clear from Table 3 that good iron loss properties (building factor) were obtained for the samples according to the present disclosure (grain-oriented electrical steel sheets).

Claims

1. A grain-oriented electrical steel sheet comprising a base steel sheet containing Si: 1.50 mass% to 8.00 mass%, Mn: 0.02 mass% to 1.00 mass%, and Co: 0.005 mass% to 0.050 mass%, and a base film mainly composed of forsterite, formed on the surface of the base steel sheet, wherein

Ti content in the base steel sheet and the base film as a whole is 0.0050 mass% to 0.0200 mass%, and the following expression (1) is satisfied, where R17 is the ratio of hysteresis loss Wh_{17} to iron loss $W_{17/50}$ when excited at 1.7 T and R19 is the ratio of hysteresis loss Wh_{19} to iron loss $W_{19/50}$ when excited at 1.9 T,

$$0.30 \leq R17 \leq R19 \qquad \ldots(1).$$

2. The grain-oriented electrical steel sheet according to claim 1, wherein Ti content in the base steel sheet is 0.0030 mass% or less.

3. The grain-oriented electrical steel sheet according to claim 1 or 2, further comprising an insulating coating on the surface of the base film.

4. The grain-oriented electrical steel sheet according to any one of claims 1 to 3, wherein the base steel sheet further contains one or more selected from the group consisting of Sn: 0.500 mass% or less, Cr: 0.500 mass% or less, Cu: 0.50 mass% or less, Ni: 0.50 mass% or less, Bi: 0.500 mass% or less, P: 0.500 mass% or less, Sb: 0.500 mass% or less, Mo: 0.500 mass% or less, B: 25.0 mass ppm or less, Nb: 0.020 mass% or less, V: 0.020 mass% or less, As: 0.0200 mass% or less, Zn: 0.020 mass% or less, Pb: 0.0100 mass% or less, W: 0.0100 mass% or less, Ga: 0.0050 mass% or less, and Ge: 0.0050 mass% or less.

FIG. 1

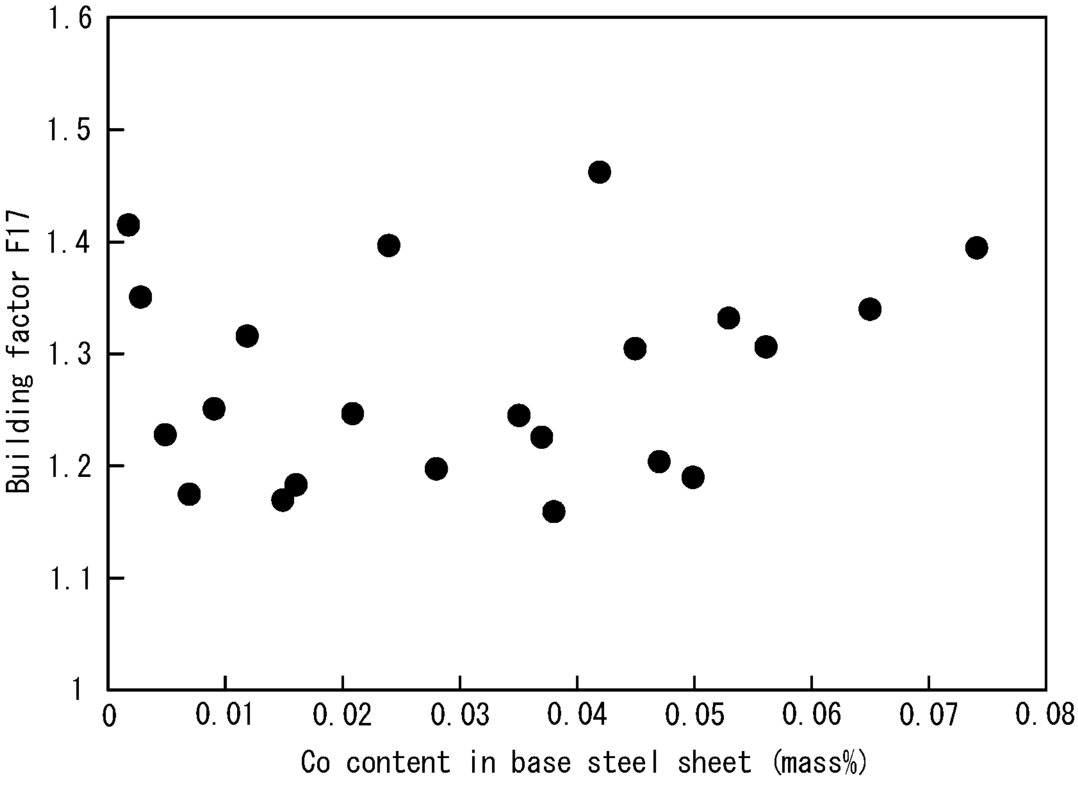
1.6
1.5
1.4
1.3
1.2
1.1
1
Building factor F17
0
0.01
0.02
0.03
0.04
0.05
0.06
0.07
0.08
Co content in base steel sheet (mass%)

FIG. 2

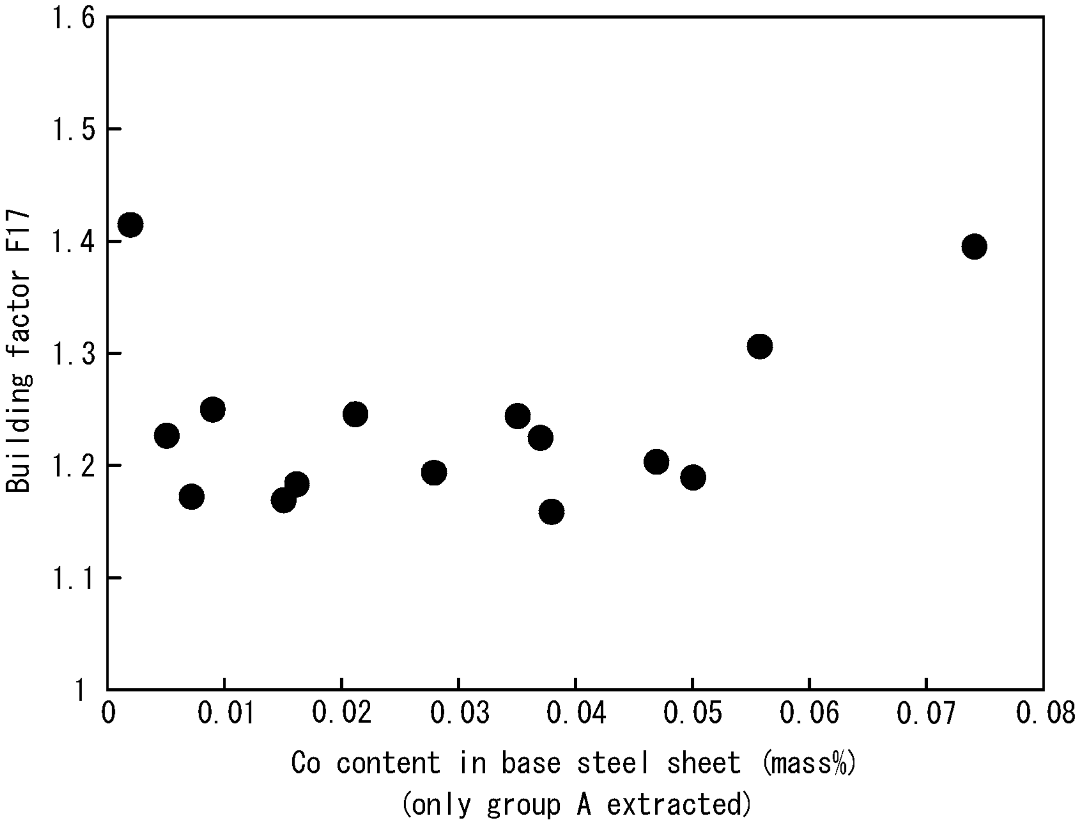
1.6
1.5
1.4
1.3
1.2
1.1
1
Building factor F17
0
0.01
0.02
0.03
0.04
0.05
0.06
0.07
0.08
Co content in base steel sheet (mass%)
(only group A extracted)

FIG. 3

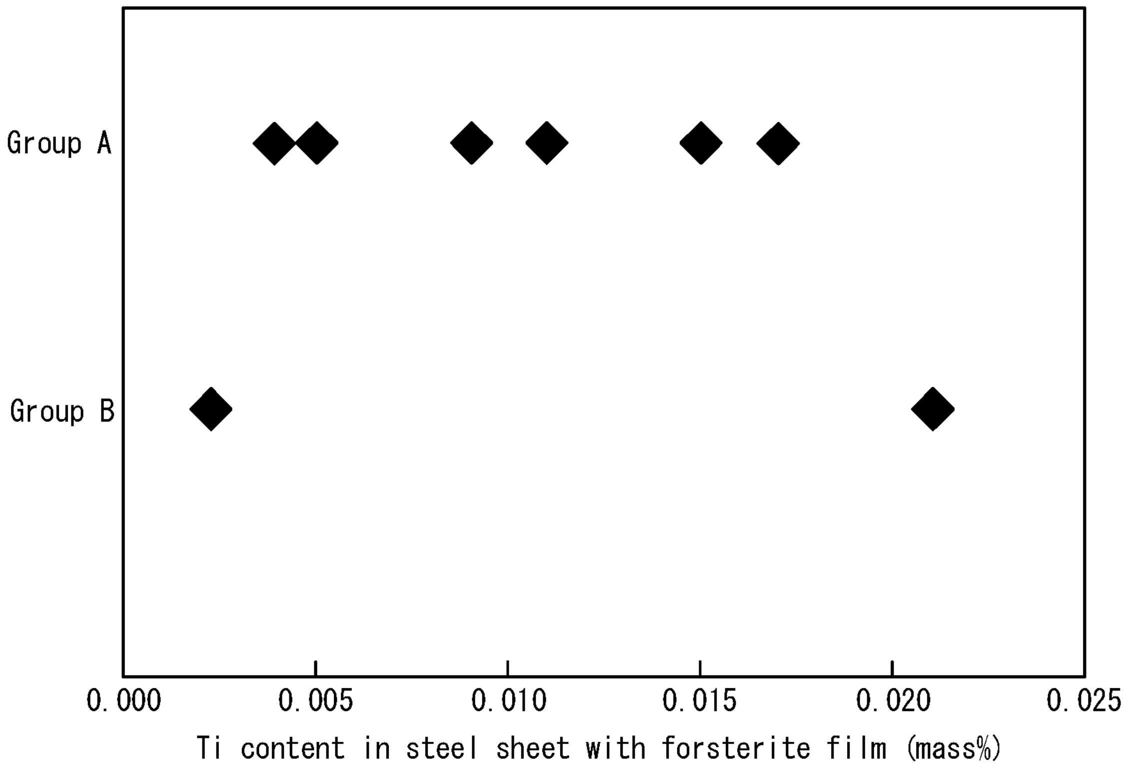
Group A
Group B
0.000
0.005
0.010
0.015
0.020
0.025
Ti content in steel sheet with forsterite film (mass%)

FIG. 4

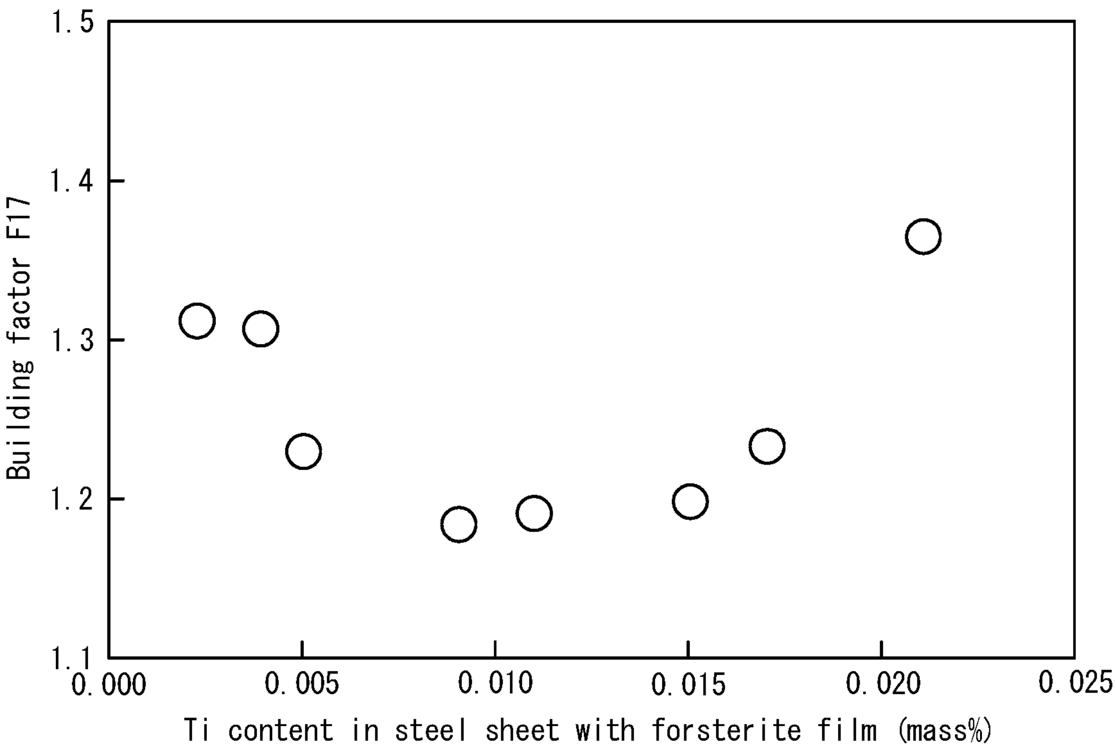
1.5
1.4
1.3
1.2
1.1
Building factor F17
0.000
0.005
0.010
0.015
0.020
0.025
Ti content in steel sheet with forsterite film (mass%)

INTERNATIONAL SEARCH REPORT

International application No.
PCT/JP2023/032247

A. CLASSIFICATION OF SUBJECT MATTER

C21D 8/12(2006.01)n; ***C22C 38/00***(2006.01)i; ***C22C 38/10***(2006.01)i; ***C22C 38/14***(2006.01)i; *C22C 38/60*(2006.01)n; ***H01F 1/147***(2006.01)i
FI: C22C38/00 303U; C22C38/10; C22C38/14; H01F1/147 183; C22C38/60; C21D8/12 B

According to International Patent Classification (IPC) or to both national classification and IPC

B. FIELDS SEARCHED

Minimum documentation searched (classification system followed by classification symbols)

C21D8/12; C21D9/46; C22C38/00-C22C38/60; H01F1/147

Documentation searched other than minimum documentation to the extent that such documents are included in the fields searched

Published examined utility model applications of Japan 1922-1996
Published unexamined utility model applications of Japan 1971-2023
Registered utility model specifications of Japan 1996-2023
Published registered utility model applications of Japan 1994-2023

Electronic data base consulted during the international search (name of data base and, where practicable, search terms used)

C. DOCUMENTS CONSIDERED TO BE RELEVANT

Category*	Citation of document, with indication, where appropriate, of the relevant passages	Relevant to claim No.
A	JP 9-291313 A (KAWASAKI STEEL CORP.) 11 November 1997 (1997-11-11) entire text, all drawings	1-4
A	JP 2012-92409 A (JFE STEEL CORP.) 17 May 2012 (2012-05-17) entire text, all drawings	1-4
A	JP 2013-136824 A (JFE STEEL CORP.) 11 July 2013 (2013-07-11) entire text, all drawings	1-4
A	JP 2021-123766 A (NIPPON STEEL CORP.) 30 August 2021 (2021-08-30) entire text, all drawings	1-4
A	JP 2006-274405 A (JFE STEEL CORP.) 12 October 2006 (2006-10-12) entire text, all drawings	1-4
A	CN 108456829 A (HEFEI SHANGQIANG ELECTRIC TECHNOLOGY CO., LTD.) 28 August 2018 (2018-08-28) entire text	1-4

☐ Further documents are listed in the continuation of Box C. ☑ See patent family annex.

* Special categories of cited documents:
"A" document defining the general state of the art which is not considered to be of particular relevance
"E" earlier application or patent but published on or after the international filing date
"L" document which may throw doubts on priority claim(s) or which is cited to establish the publication date of another citation or other special reason (as specified)
"O" document referring to an oral disclosure, use, exhibition or other means
"P" document published prior to the international filing date but later than the priority date claimed
"T" later document published after the international filing date or priority date and not in conflict with the application but cited to understand the principle or theory underlying the invention
"X" document of particular relevance; the claimed invention cannot be considered novel or cannot be considered to involve an inventive step when the document is taken alone
"Y" document of particular relevance; the claimed invention cannot be considered to involve an inventive step when the document is combined with one or more other such documents, such combination being obvious to a person skilled in the art
"&" document member of the same patent family

Date of the actual completion of the international search	Date of mailing of the international search report
10 November 2023	**21 November 2023**

Name and mailing address of the ISA/JP	Authorized officer
Japan Patent Office (ISA/JP) **3-4-3 Kasumigaseki, Chiyoda-ku, Tokyo 100-8915** **Japan**	Telephone No.

Form PCT/ISA/210 (second sheet) (January 2015)

INTERNATIONAL SEARCH REPORT
Information on patent family members

International application No.
PCT/JP2023/032247

Patent document cited in search report	Publication date (day/month/year)	Patent family member(s)	Publication date (day/month/year)
JP 9-291313 A	11 November 1997	(Family: none)	
JP 2012-92409 A	17 May 2012	(Family: none)	
JP 2013-136824 A	11 July 2013	US 2015/0248957 A1 entire text, all drawings WO 2013/099281 A1 EP 2799572 A1 CN 104024454 A KR 10-2014-0102689 A RU 2572935 C1	
JP 2021-123766 A	30 August 2021	(Family: none)	
JP 2006-274405 A	12 October 2006	(Family: none)	
CN 108456829 A	28 August 2018	(Family: none)	

Form PCT/ISA/210 (patent family annex) (January 2015)

REFERENCES CITED IN THE DESCRIPTION

This list of references cited by the applicant is for the reader's convenience only. It does not form part of the European patent document. Even though great care has been taken in compiling the references, errors or omissions cannot be excluded and the EPO disclaims all liability in this regard.

Patent documents cited in the description

- JP S4015644 B **[0008]**
- JP S5113469 B **[0008]**
- JP 2000129356 A **[0008]**
- JP S572252 B **[0008]**
- JP H0672266 B **[0008]**
- JP 2021509149 A **[0032]**